

01 Oct 2007

## Phase Transformations of Calcium Phosphates Formed in Wet Field Environments

O. M. Clarkin


Mark R. Towler

*Missouri University of Science and Technology*, mtowler@mst.edu

G. M. Insley

M. E. Murphy

Follow this and additional works at: [https://scholarsmine.mst.edu/che\\_bioeng\\_facwork](https://scholarsmine.mst.edu/che_bioeng_facwork)

 Part of the [Biochemical and Biomolecular Engineering Commons](#), and the [Biomedical Devices and Instrumentation Commons](#)

---

### Recommended Citation

O. M. Clarkin et al., "Phase Transformations of Calcium Phosphates Formed in Wet Field Environments," *Journal of Materials Science*, vol. 42, no. 19, pp. 8357 - 8362, Springer, Oct 2007.

The definitive version is available at <https://doi.org/10.1007/s10853-006-0783-3>

This Article - Journal is brought to you for free and open access by Scholars' Mine. It has been accepted for inclusion in Chemical and Biochemical Engineering Faculty Research & Creative Works by an authorized administrator of Scholars' Mine. This work is protected by U. S. Copyright Law. Unauthorized use including reproduction for redistribution requires the permission of the copyright holder. For more information, please contact [scholarsmine@mst.edu](mailto:scholarsmine@mst.edu).

# Phase transformations of calcium phosphates formed in wet field environments

O. M. Clarkin · M. R. Towler · G. M. Insley ·  
M. E. Murphy

Received: 31 May 2006 / Accepted: 10 August 2006 / Published online: 22 March 2007  
© Springer Science+Business Media, LLC 2007

**Abstract** The crystal phase and morphology of calcium phosphate salts precipitated in a wet field environment at temperatures between 30 and 70 °C and pHs between 3 and 8 were examined. Dicalcium Phosphate Dihydrate (DCPD) was the most prevalent phase precipitated. Using accelerated ageing study techniques, precipitates studied were aged, under dry conditions at 50 °C for 8 and 16 days, before being re-examined using XRD, FTIR and SEM techniques. DCPD was found to be most stable when precipitated at 40 °C and 5 pH. Considerably more phase transformation to Octacalcium Phosphate (OCP), Amorphous Calcium Phosphate (ACP) and Hydroxyapatite (HA) was seen at high temperatures and high pHs, and a greater tendency to form anhydrous salts was seen at high temperatures and low pHs. Using techniques such as XRD, FTIR and SEM the transformation of the DCPD precipitate to OCP was analysed and appeared to occur without the presence of an intermediate amorphous phase. However, transformation from OCP to HA did result in the formation of an intermediate amorphous phase.

## Introduction

Bone formation and growth involves the precipitation of calcium phosphate in the form of Hydroxyapatite (HA,

$\text{Ca}_5(\text{PO}_4)_3(\text{OH})$ ) [1]. HA has been the subject of extensive research and, as a result, the other calcium phosphate salts have been marginalised [2]. Dicalcium Phosphate Dihydrate (DCPD,  $\text{CaHPO}_4 \cdot 2\text{H}_2\text{O}$ ), Octacalcium Phosphate (OCP,  $\text{Ca}_8\text{H}_2(\text{PO}_4)_6 \cdot 5\text{H}_2\text{O}$ ) and Amorphous Calcium Phosphate (ACP) have often been observed as precursor phases to HA [3, 4]; naturally being hydrolysed to HA in an aqueous environment [5]. The mechanism of this transformation is crucial in understanding precipitation of natural bone mineral [6]. Many of these calcium phosphate phases are used in medical devices and their stability is thus very important to the industry. Incorrect production or storage of these phases may lead to premature product failure [7, 8]. For example, DCPD, a component of many calcium phosphate cements [7, 9–11], can transform to Dicalcium Phosphate Anhydrous (DCPA,  $\text{CaHPO}_4$ ) when aged [8]. The crystallographic alterations occurring with this transformation, as well as the effects of varying formation temperature and pH of the initial precipitate have not previously been investigated.

Precipitation of calcium phosphates from solution involves the control of a number of different parameters. Any phase precipitated from a solution saturated with both calcium and phosphate ions is dependent on factors, including relative concentrations of ions, ionic strength, pH and temperature of the solution [1, 3, 12, 13]. The phase precipitated can be predicted with knowledge of these parameters but accurate calculation can be compromised due to the complication of heterogeneous nucleation on initial precipitates [14].

Spontaneous precipitation requires a high degree of super saturation in the solution, but does result in unbiased precipitation [11, 3]. The aim of this paper is to outline the formation of some calcium phosphate phases under a set range of temperatures and pHs in order to better understand

O. M. Clarkin · M. R. Towler (✉)  
Materials & Surface Science Institute, University of Limerick,  
Limerick, Ireland  
e-mail: mark.towler@ul.ie

G. M. Insley · M. E. Murphy  
Biomaterials Research Group, Stryker, Limerick, Ireland

the phase transformations that occur between phases. In this study, ionic strength, concentration and Ca:P ratio of solutions were kept constant, with the pH and temperature being the only variables. Nucleating agents were not added, allowing precipitation to occur spontaneously.

## Materials and methods

A calcium phosphate solution (Ca:P, 1) was synthesised by mixing 43.5 g Calcium Acetate–H<sub>2</sub>O ((CH<sub>3</sub>COO)<sub>2</sub>Ca·½H<sub>2</sub>O), 30 g Ammonium Dihydrogen Phosphate (NH<sub>4</sub>H<sub>2</sub>PO<sub>4</sub>) (both Ocon Chemicals Ltd., Ireland) and 1,600 mL deionised water [15] under constant stirring of 500 rpm using a magnetic stirrer. A calibrated hotplate controlled the temperature of solution. The pH of the precipitate solution was regulated using hydrochloric acid (HCl, Reagacon Ltd., Ireland) for pHs below 4 and Ammonium hydroxide (NH<sub>4</sub>OH, Reagacon Ltd., Ireland) for pHs above 4 [13, 15]. Solutions were heated to temperatures of 30, 40, 50, 60 and 70 °C prior to precipitation and pHs of the precipitates were adjusted to 3, 4, 5, 6, 7 and 8 after precipitation. Separate solutions were prepared for each temperature/pH data set. Once the desired temperature and pH was achieved, the precipitated solution was allowed to equilibrate for 1 hour. During this dwell time, ammonium hydroxide was added, if required to maintain the pH [12]. All chemicals used for the study were of analytical grade.

Solutions were subsequently filtered through a Büchner funnel under vacuum. Precipitates were subjected to two washes with deionised water (ca. 500 mL per wash) and a final wash in 70/30 Isopropanol/water solution (ca. 250 mL) [15, 6]. Precipitates were left to dry (room temperature, 24 h). Each powder was then divided into four samples for independent XRD, FTIR, SEM and ageing studies.

X-ray Diffraction was performed using a Rigaku X-ray diffractometer (Rigaku, Japan) with analytical diffraction software. Data collection was performed in the  $2\theta$  range from 2° to 35° (using a scan step of 0.04°  $2\theta$  every 2 s), using Cu  $K_{\alpha}$  radiation ( $\lambda = 0.15406$  nm), with an anode current of 40 mA and a tube voltage of 40 kV [5]. XRD analysis was performed on the precipitates after drying. Each sample was subsequently aged at 50 °C for 8 and 16 days, consecutively. Samples selected for ageing were packaged in sealed sample bags filled with a silica desiccant (to absorb free moisture). Joint committee powder diffraction file (JCPDF) patterns were used to identify the phases present in the powders.

Fourier Transformation Infrared Spectroscopy (FTIR) was performed using a Nicolet Magna 550 FTIR spectrometer (LDS Nicolet, USA). About 2 mg of each

precipitate was mixed with 300 mg of potassium bromide (KBr) and then pressed (10 tonnes) to produce a disc [6]. Discs were analysed at room temperature in transmission mode. The resolution was 4 cm<sup>-1</sup>. The resultant spectra were compared to relevant literature [2, 3, 5, 9, 15, 16].

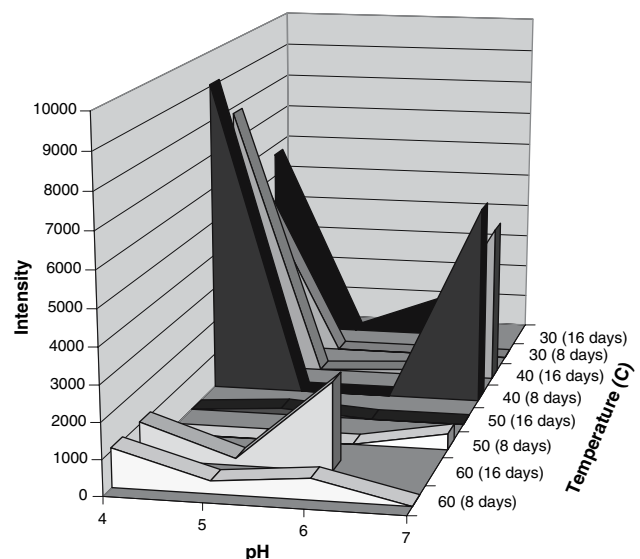
Scanning Electron Microscopy was performed using a Jeol JSM 840 microscope (Jeol, Japan). SEMs were taken at magnification range of 200× to 5,000×, all at 20 kV. The samples required gold sputtering prior to analysis. Resultant micrographs were compared, both with one another and with the literature [2, 3, 5, 13, 15, 16].

## Results and discussion

### 30 and 40 °C precipitates

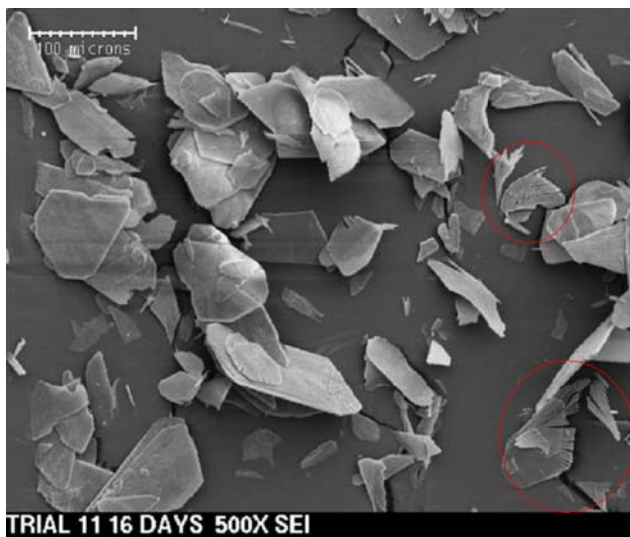
The XRD plots for the powders precipitated at 30 and 40 °C were found to correspond to that of DCPD (JCPDS 9-77). The FTIR spectra of these samples all exhibit similar absorption peaks to one another. Bound water peaks, as well as OH, PO<sub>4</sub> and HPO<sub>4</sub> stretching peaks [1] can be distinguished from the spectra. SEM micrographs of powders precipitated at 30 and 40 °C show crystals consisting of both interlocking and individual platelets (Fig. 4A, B). This is typical of DCPD morphology [13, 17].

Figure 1 shows the relative degradation of powders precipitated at various temperatures and pHs. DCPD precipitated at 30 °C, at pH 4 exhibits a peak at 26.5°  $2\theta$  on the XRD trace after 8 days ageing (Fig. 5F), implying considerable conversion to DCPA [3]. None of the other powders precipitated at this temperature showed signs of



**Fig. 1** DCPA (JCPDS: 9-80) peak intensity (at 26.5°  $2\theta$ ) for powders aged for 8 and 16 days

ageing after 8 days. As can be seen from Fig. 5G, C, after 16 days ageing, the precipitates formed at 30 °C, 4 pH and 30 °C, 6 pH exhibited considerable degradation. Those precipitated at 30 °C, 5 pH showed no degradation as can be seen from Fig. 5D. As visible from Fig. 5A, B powders precipitated at 40 °C showed considerable degradation after 8 days, at the higher and lower ends of the pH spectrum but no degradation at 5 and 6 pH. After 16 days ageing, powders precipitated at 40 °C again showed heavy degradation at the upper and lower ends of the pH spectrum, whereas powders precipitated at 40 °C, 5 pH showed no degradation. SEM analysis of degraded DCPD showed a break down of the DCPD interconnected platelet forma-



**Fig. 2** SEM micrograph of DCPD particles, formed at 40 °C, 4 pH, aged for 16 days

tions into individual platelets, followed by splitting of the individual platelets. This has been highlighted in Fig. 2.

### 50 °C precipitates

Powders precipitated at 50 °C at 4, 5 and 6 pH have similar diffraction patterns to the DCPD powders precipitated at 30 and 40 °C. The FTIR spectra are also similar, showing no variation in the absorbance peaks between powders precipitated at 50 °C at the lower pHs and those powders precipitated at 30 and 40 °C. Powder precipitated at 7 pH exhibits some decreased crystallinity yet a distinct DCPD pattern is still evident which has a slight tendency towards OCP. This is evidenced by the peak at 4.7° 2θ corresponding to the 100% OCP peak (JCPDS 26-1056) as seen in Fig. 3A. Powder precipitated at 8 pH has a similar XRD pattern but without any DCPD peaks present, leaving HA/OCP-type phase being detected (Fig. 3D). The FTIR spectra also confirm this DCPD → OCP → HA transition. At 7 pH the initial bound water/OH stretching absorbance peak [3,540 cm<sup>-1</sup>, 3,100 cm<sup>-1</sup>] [2] has broadened and many of the PO<sub>4</sub> stretching peaks have disappeared [550–600 cm<sup>-1</sup>, 960 cm<sup>-1</sup>, 1,020–1,120 cm<sup>-1</sup>] [2]. This is most likely due to an increase in the Ca:P ratio of the powder and a removal of the bound water from the DCPD [2, 8, 16]. At 8 pH, the FTIR spectrum shows further decreases in bound water, OH and PO<sub>4</sub> related peaks, as would be expected from a transformation from DCPD → OCP → HA.

After 8 days ageing, there is a reduction of the DCPD peaks of the powder precipitated at 4 pH. The XRD patterns appear similar after 16 days, however there is a reduction in the 100% DCPD peak at 11.60° 2θ in all powders except those precipitated at 6 pH and 7 pH.

**Fig. 3** XRD plot of phases precipitated at 50 and 60 °C. Where; (A) corresponds to precipitates formed at 70 °C and 5 pH, (B) at 60 °C and 7 pH, (C) at 60 °C and 6 pH, (D) at 50 °C and 7 pH, (E) at 60 °C and 8 pH

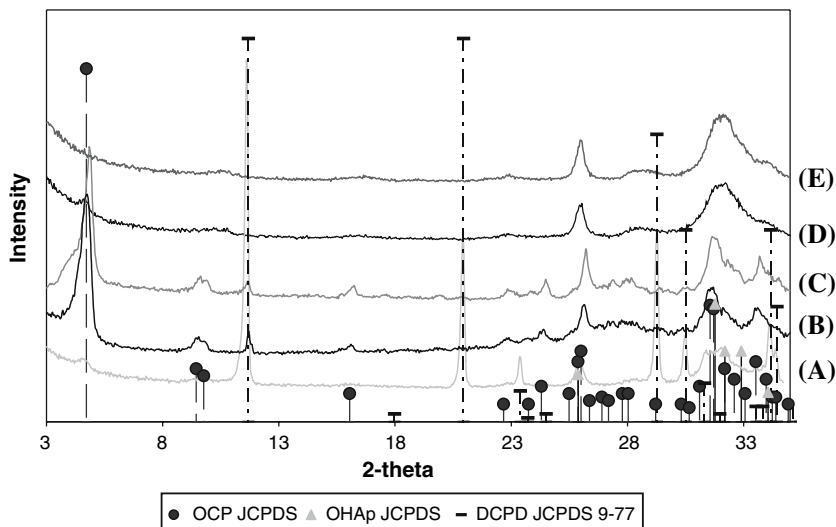
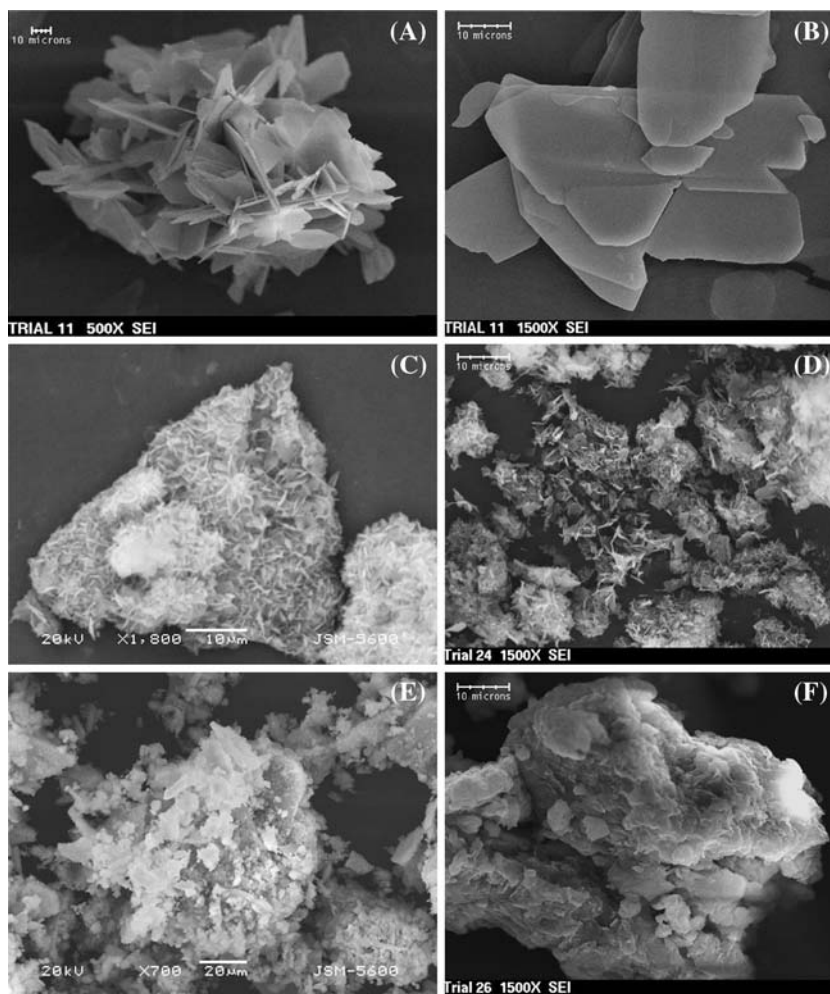


**Fig. 4** SEM micrographs of powders precipitated at; (A) 40 °C, 4 pH (500× mag.), (B) 40 °C, 4 pH (1,500× mag.), (C) 60 °C, 6 pH (1,800× mag.), (D) 60 °C, 7 pH (1,500× mag.), (E) 60 °C, 8 pH (700× mag.), (F) 70 °C, 6 pH (1,500× mag.)



#### 60°C precipitates

At 60 °C, the lower pH precipitates are DCPD (JCPDS 9-77). However, powders precipitated at 4 pH and 5 pH also have a small DCPA content. Powders precipitated at 6, 7 and 8 pH are largely amorphous. Figure 3C shows powder

precipitated at 6 pH. The crystal phase is mostly OCP with some DCPD present, denoted by the presence of a peak at 11.7° 2θ. FTIR analysis shows a standard OCP/HA spectrum, with no evidence of bound water and minimum PO<sub>4</sub> stretching peaks. The SEM micrograph (Fig. 4C) shows curved plate-type growth, approx. 1–5 µm in length and

**Fig. 5** XRD of precipitates formed at (A) 40 °C, 7 pH; (B) 40 °C, 4 pH; (C) 30 °C, 6 pH; (D) 30 °C, 5 pH; (E) 60 °C, 6 pH, (F) 30 °C, 4 pH and (G) 30 °C, 4 pH and aged at 50 °C for (A) 8 days, (B) 8 days, (C) 16 days, (D) 16 days, (E) 16 days, (F) 8 days, (G) 16 days

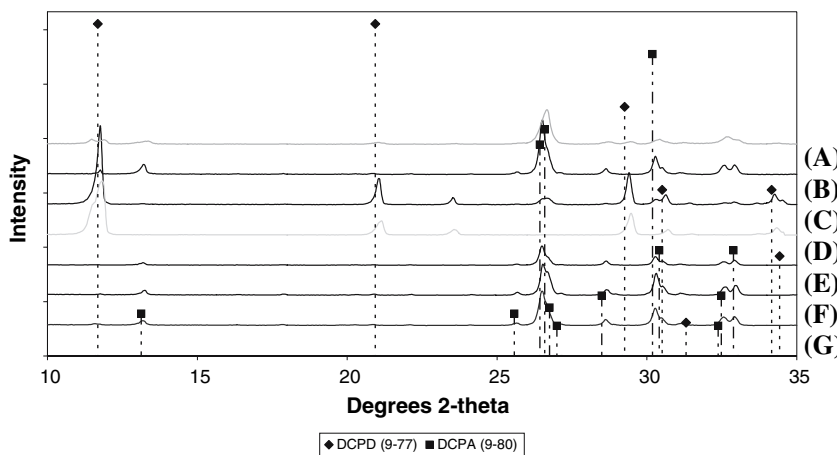
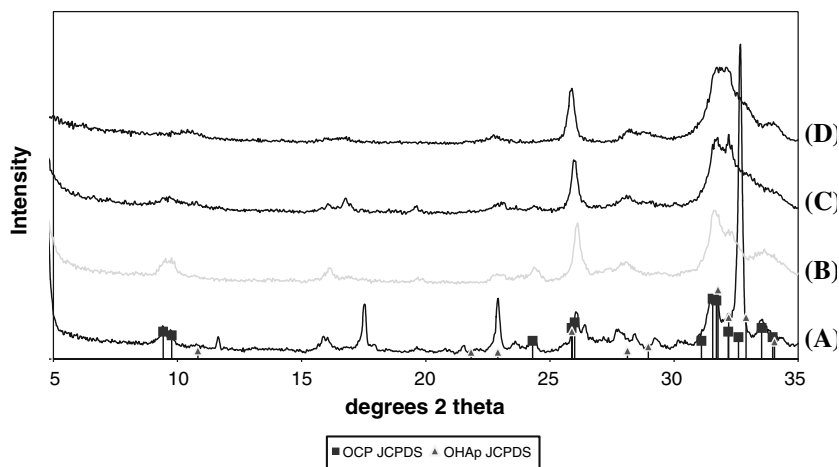


**Fig. 6** XRD plot of calcium phosphates precipitated at 70 °C and 5 pH (A), 6 pH (B), 7 pH (C) and 8 pH (D)

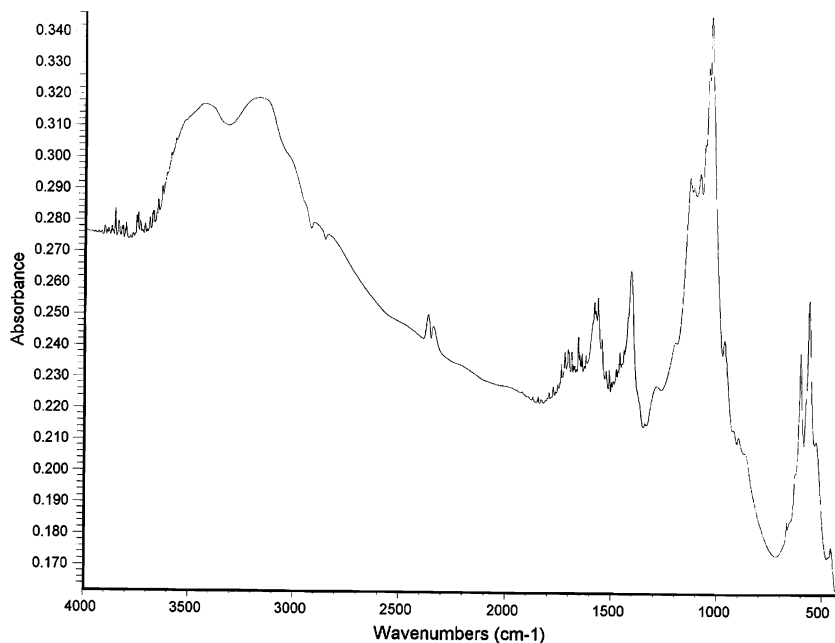


0.01  $\mu\text{m}$  in width. This growth appears to have agglomerated onto larger particles in most areas (Fig. 4C). Figure 3B shows the XRD plot of powder precipitated at 7 pH. This powder is similar to that precipitated at 6 pH, still with a small amount of DCPD present, but showing higher relative quantities of OCP. The amorphous content has increased, evinced by a broadening of the peaks. The FTIR spectrum exhibits standard HA/OCP type absorbance peaks. The SEM micrographs of this powder (Fig. 4D) show a sharp edged plate-like morphology with no larger organization seen in Fig. 4C. Powder precipitated at 8 pH yields an XRD pattern akin to HA (Fig. 3E) but with low intensities implying that the powder is largely amorphous. The FTIR spectra are similar to standard HA/OCP spectra [13]. The SEM micrographs (Fig. 4E) show agglomerate formation, similar to ACP [13] but also exhibit some elongated

formations characteristic of HA morphology [2]. Examination of the amorphous areas at higher magnifications (5,000 $\times$ ) reveals no microstructure that would have been indicative of a crystal structure finer than that already observed. This lack of crystal structure appears to be a semi-amorphous intermediate transition phase, which is occurring as the morphology transforms from OCP type platelet morphology to a needle like HA morphology.

After 8 days ageing, a reduction in the 100% peak of DCPD occurs for the powder precipitated at 4 pH alongside a relative increase in intensity of the DCPA peak at  $26.5^\circ 2\theta$ . No change can be seen in the other powders precipitated at 60 °C. After 16 days of ageing at 50 °C, there are no changes evident in powders precipitated at 4 and 5 pH but, as can be seen from Fig. 5E, there is an increase in the peak at  $26.5^\circ 2\theta$  in the powder precipitated at 6 pH. This

**Fig. 7** FTIR trace of the unidentified phase precipitated at 70 °C and 5 pH



may be due to the ageing of the DCPD element of this powder.

#### 70 °C precipitates

Powder precipitated at 3 pH was comprised of approximately 50:50 DCPA:DCPD. In the corresponding micrograph, cluster type spirals are dispersed amongst platelets of DCPD. Powder precipitated at 4 pH exhibited crystallinity corresponding to DCPD. The micrograph of the 4 pH precipitate however shows only the presence of DCPD plates with no interaction between them. Precipitates formed at 5, 6, 7 and 8 pH exhibit lower peak intensities compared to other precipitates, incurring a lower degree of crystallinity. In Fig. 6A, showing the diffraction pattern of powder precipitated at 5 pH, a considerable amount of OCP phase is evident, as well as HA. However, there is a 100% peak at  $32.7^\circ 2\theta$ , which, as of yet, has not been identified. At 6 pH, the unidentified phase has almost disappeared from the XRD plot and a mixture of HA and OCP is evident, with HA being dominant. A distinct change in the FTIR spectrum can be seen from Fig. 7; the unidentified phase formed at 5 pH resulting in a dramatic rise in the bound water and OH groups while still having a reduction in the  $\text{HPO}_4$  and  $\text{PO}_4$  groups when compared to the DCPD type spectrum, as seen in the 4 pH precipitate. The FTIR spectrum has elements of both an acidic (DCPD) precipitate and an alkaline precipitate (HA). The spectrum of the powder precipitated at 6 pH, however, shows classic HA/OCP type absorption peaks. From the micrograph of this precipitate (Fig. 4F), powder agglomerates are seen, with no evidence of crystallites (even at 5,000 $\times$ ). A reduction in OCP content relative to HA can be seen going from 6 pH to 8 pH, with no OCP peaks visible at 8 pH. No difference between these powders is evident from FTIR analysis.

Ageing of the powders precipitated at 70 °C had minimal effect, with only a reduction in the 100% DCPD peak in the powder precipitated at 50 °C, 3 pH after 16 days. No variation was seen in the other powders, as DCPD content of these powders was minimal.

## Conclusion

Calcium phosphate salts precipitated in a wet field, at temperatures between 30 and 70 °C in acidic to neutral solutions, were examined by a variety of characterization techniques. DCPD was the most prevalent phase precipitated, with the most stable precipitates being produced at 50 °C, 5 pH. Upon accelerated ageing of these powders, DCPD platelets separated and split, forming a dehydrated powder with a crystal structure similar to DCPA. In the higher pH region of precipitation, DCPD converted to OCP, presumably by means of surface dissolution and re-precipitation. An intermediate phase was also recorded as DCPD was re-precipitated as HA at high temperatures. This phase was crystalline with its orientation at  $32.7^\circ 2\theta$ .

## References

- Christoffersen MR, Dohrup J, Christoffersen J (1998) *J Cryst Growth* 186:283
- Raynaud S, Champion E, Bernache-Assollant D, Thomas P (2002) *Biomaterials* 23:1065
- Arifuzzaman SM, Rohani S (2004) *J Cryst Growth* 267:624
- Grossl PR, Inskeep WP (1992) *Geochim Cosmochim Acta* 56:1955
- Zhang H, Yan Y, Wang Y, Li S (2003) *Mat Res* 6(1):111
- Graham S, Brown PW (1993) *J Cryst Growth* 132:215
- Ishikawa K, Takagi S, Chow LC, Yoshiko I (1995) *J Mater Sci – Mater Med* 6:528
- Landin M, Rowe RC, York P (1994) *Eur J Pharmacol Sci* 2:245
- Miyamoto Y, Ishikawa K, Takechi M, Toh T, Yoshida Y, Nagayama M, Kon M, Asaoka K (1997) *J Biomed Mater Res* 37(4):457
- Costantino PD, Friedman CD, Chow LC, Takagi S (1991) *Mater Res Soc Symp Proc* 179:3
- Grover LM, Gbureck U, Wright AJ, Tremayne M, Barralet JE (2006) *Biomaterials* 27:2178
- Montastruc L, Azzaro-Pantel C, Biscans B, Cabassud M, Domenech S (2003) *Chem Eng J* 94:41
- Christoffersen J, Christoffersen MR, Kibalczyk W, Flemming W, Andersen A (1989) *J Cryst Growth* 94:767
- Freche M, Heughebaert JC (1989) *J Cryst Growth* 94:947
- Pang X, Bao X (2002) *J Eur Ceramics Soc* 23:1697
- Joshi VS, Joshi MJ (2003) *Cryst Res Technol* 38(9):817
- Ferreira A, Oliveira C, Rocha F (2003) *J Cryst Growth* 252:599